Volume 1 | Number 1 | Jan 2013 | Pages 1–100

Journal of
Materials Chemistry A

Materials for energy and sustainability
www.rsc.org/materialsA

ROYAL SOCIETY
OF CHEMISTRY

ROYAL SOCIETY
OF CHEMISTRY

www.rsc.org/materialsA

Journal Name

ARTICLE

Highly efficient photocatalytic conversion of CO$_2$ into solid CO using H$_2$O as a reductant over Ag-modified ZnGa$_2$O$_4$†

Zheng Wang,[a] Kentaro Teramura,*[abc] Saburo Hosokawa[ab] and Tsunehiro Tanaka*[ab]

Highly crystalline spinel phase ZnGa$_2$O$_4$ modified with a Ag cocatalyst exhibited high activity and selectivity toward CO evolution in the photocatalytic conversion of CO$_2$ using H$_2$O as a reductant under UV light irradiation. The stoichiometric evolution of CO, H$_2$, and O$_2$ clearly indicated that H$_2$O worked as an electron donor for the photoreduction of CO$_2$. Highly crystalline ZnGa$_2$O$_4$ was synthesized by the solid-state reaction method at a calcination temperature as low as 973 K. Upon optimizing the fabrication conditions, such as calcination temperature and duration, the photocatalytic activity of ZnGa$_2$O$_4$ was maximized because of optimum balance between crystallinity and surface area in the catalyst material. Furthermore, the formation of metallic Ag particles with different sizes and dispersions on the surface of ZnGa$_2$O$_4$ influenced the evolution of CO. When Ag nanoparticles were loaded onto the ZnGa$_2$O$_4$ calcined at 1123 K for 40 h using the chemical reduction method, the highest formation rates of CO, H$_2$, and O$_2$ (155.0, 8.5, and 74.3 µmol h^{-1}, respectively) were obtained, and the selectivity toward CO evolution reached 95.0%. An isotope-labeling experiment using ^{13}CO$_2$ confirmed that the origin of the evolved CO was not from organic contamination but from the CO$_2$ gas introduced during the reaction process.

Introduction

Owing to the large global consumption of fossil fuels, the emission of greenhouse gases, such as CO$_2$, has resulted in an increase in their atmospheric concentration and an accelerated rise of global temperatures.[1-3] Growing concern about environmental problems has driven researchers to seek control of the atmospheric level of CO$_2$ through capture and storage.[2,3] From the viewpoint of the global carbon cycle, the catalytic conversion of CO$_2$ to liquid fuels and chemicals, utilizing CO$_2$ as a natural resource, is an attractive technology.[3,4] The recycling of CO$_2$ into fuels usually requires an extremely high energy input and a large supply of reductant, such as H$_2$ or CH$_4$.[3,4] Using solar light as an energy source and H$_2$O as a reductant, both of which are highly abundant, the photocatalytic conversion of CO$_2$ into useful chemical products such as CO, HCOOH, HCHO, CH$_3$OH, and CH$_4$ under ambient temperature and pressure would be a renewable and environmentally beneficial process.[3,5-8]

The photocatalytic conversion of CO$_2$ by H$_2$O, which can be regarded as artificial photosynthesis, is an uphill reaction making use of electrons generated by light energy.[5,8] The generation of H$_2$ from the reduction of protons usually competes for the photo-excited electrons and takes precedence over the reduction of CO$_2$, because the redox potential of H$^+$/H$_2$ (−0.41 V vs. NHE, at pH 7) is more positive than that of CO/CO$_2$ (−0.51 V vs. NHE, at pH 7).[9] In order to achieve the

conversion of CO$_2$ rather than the production of H$_2$ by H$_2$O over heterogeneous photocatalysts, it is extremely important to improve the selectivity of generated electrons toward the reduction of CO$_2$.[10,11] Moreover, a stoichiometric amount of O$_2$ should be evolved if H$_2$O functions efficiently as an electron donor.[10,11] Although various metal oxide photocatalysts have been reported for CO$_2$ reduction in H$_2$O, only a few materials, i.e., Zn-doped Ga$_2$O$_3$,[10] ALa$_4$Ti$_4$O$_{15}$ (where A = Ca, Sr and Ba),[11] and La$_2$Ti$_2$O$_7$,[12] showed higher selectivity for CO$_2$ reduction and simultaneously produced O$_2$ stoichiometrically. Therefore, the development of more active photocatalysts for the conversion of CO$_2$ using H$_2$O as a reductant is imperative.

It is known that the spinel type oxide ZnGa$_2$O$_4$, with a wide band gap of 4.4-5.0 eV, can efficiently decompose H$_2$O into H$_2$ and O$_2$, without any sacrificial reagents, under UV irradiation.[13] Since the reduction of CO$_2$ requires a reduction potential higher than that of H$^+$, the wide band gap of ZnGa$_2$O$_4$, which is capable of generating photoelectrons with a high reduction potential, should result in the efficient reduction of CO$_2$. Indeed, ZnGa$_2$O$_4$ possessing various morphologies, such as mesoporous,[14] nanocube,[15] and ultrathin nanosheet,[16] has been studied in the photocatalytic reduction of CO$_2$ with H$_2$O. However, the conversion efficiency of CO$_2$ in these studies was still low, and a stoichiometric amount of O$_2$ was not generated in these reactions. In addition, high crystallinity in a photocatalyst has a positive effect on its activity due to the elimination of defects, which usually act as recombination

centers for photogenerated pairs.[17,18] Research in this area reports that temperatures above 1273 K are necessary for the synthesis of $ZnGa_2O_4$ by the solid-state reaction method.[13,15,19] However, in this study, we found that highly crystalline $ZnGa_2O_4$ could be produced by this method at temperatures as low as 973 K. The highest activity for the photocatalytic conversion of CO_2 using H_2O as an electron donor was obtained over $ZnGa_2O_4$ calcined below 1273 K. Furthermore, we studied the effect of a Ag cocatalyst on the overall catalytic activity of the material, and on its selectivity toward CO evolution.

Experimental

$ZnGa_2O_4$ was fabricated by a conventional solid state reaction method. A stoichiometric mixture of Ga_2O_3 (99.0%, Kojundo) and ZnO (99.0%, Wako) was ground in the presence of small amount of water as a dispersant. The slurry was mixed thoroughly for 1 h and then dried at 353 K for 1 h. The resulting mixture was calcined from 973 K to 1473 K for 5–90 h in static air. The Ag cocatalyst was introduced to the $ZnGa_2O_4$ by photodeposition, impregnation, and chemical reduction methods. The photodeposition method was employed in situ during the photocatalytic conversion of CO_2. In the impregnation method, the photocatalyst (1.5 g) was dispersed homogeneously in an aqueous $AgNO_3$ solution (2.8 mmol L^{-1}), followed by evaporation, drying, and calcination at 723 K for 2 h in a stream of dry air. For the chemical reduction method, an aqueous $NaPH_2O_2$ solution (0.40 µmol L^{-1}) was added to 50 mL of a suspension of the photocatalyst (1.5 g) containing a given amount of $AgNO_3$. After stirring at 353 K for 1.5 h, the modified photocatalyst was filtered and dried *in vacuo* at room temperature.

The structure and crystallinity of $ZnGa_2O_4$ samples were characterized by X-ray diffraction (XRD) using a Rigaku Multi Flex powder X-ray diffractometer equipped with Cu Kα (λ= 0.154056 nm) radiation, and the applied voltage and current were 30 kV and 30 mA, respectively. The sample powder was pressed into a glass holder with the area of 2 cm^2 and measured at a step width of $0.02°$ and a scan rate of 0.3 sec. N_2 adsorption at 77 K was obtained on a volumetric gas adsorption apparatus (BELmini, Bel Japan, Inc.). The $ZnGa_2O_4$ powder was pretreated at 473 K under vacuum condition for 2 h. The specific surface area of $ZnGa_2O_4$ was calculated from N_2 adsorption isotherm in the relative pressure between 0 and 0.5 using the Brunauer–Emment–Teller (BET) method. The Ag K-edge (25.5 keV) X-ray absorption fine structure (XAFS) measurements were made in fluorescence mode at the BL01B1 beamline of the SPring-8 synchrotron radiation facility (Hyogo, Japan). The spectra were reduced by a Rigaku REX2000 program Ver. 2.5.9 (Rigaku Corp.). The UV-Vis diffuse reflectance spectra (UV-Vis DRS) were measured by a JASCO Corporation V-670 spectrometer equipped with an integrating sphere. Spectralon like $BaSO_4$, supplied by Labsphere Inc. was used as a reflection standard. TEM images were obtained with a JEOL JEM-1400 transmission electron microscope (TEM) operating at an accelerating voltage of 120 kV.

The photocatalytic reaction was carried out in a flow system using an inner-irradiation-type reaction vessel at room temperature and ambient pressure. The photocatalyst (1.0 g) was dispersed in ultra-pure water (1.0 L) containing 0.1 mol of $NaHCO_3$, and CO_2 gas (99.999%) was bubbled into the solution at a flow rate of 30 mL min^{-1}. The suspension was irradiated under a 400 W high-pressure mercury lamp with a quartz filter

connected to a water cooling system. The outlet of the reactor was connected to a six-way valve with a sampling loop. Generated gaseous products such as H_2, O_2, and CO together with CO_2 gas were collected and analyzed by thermal conductivity detector-gas chromatography (TCD-GC) using a GC-8A chromatograph (Shimadzu Corp.) equipped with a Molecular Sieve 5A column with Ar as the carrier gas, and by flame ionization detector-gas chromatography (FID-GC) using a methanizer and a ShinCarbon ST column with N_2 as the carrier gas. In the isotope-labeling experiment, $^{12}CO_2$ gas was replaced by $^{13}CO_2$. The formation of ^{13}CO and ^{12}CO under photoirradiation was analyzed by a quadrupole-type mass spectrometer (BEL Japan, Inc., BEL Mass) combined with the TCD-GC using Ar as the carrier gas.

Results and Discussion

The synthesis of highly crystalline $ZnGa_2O_4$ by the solid state reaction method requires suitable thermal treatment. Fig. 1(A) and (B) show the XRD patterns of $ZnGa_2O_4$ under different calcination temperature and time. All samples calcined from 973 K to 1473 K exhibit the typical spinel structure of $ZnGa_2O_4$ (Fig. 1(A)), but there is some impurity assigned to ZnO in the case of $ZnGa_2O_4$ calcined at 973 K (Figure S1). This indicates that calcination above 973 K after the physical mixing procedure employed here successfully causes crystallization of $ZnGa_2O_4$. Moreover, all the peaks in the XRD patterns of $ZnGa_2O_4$ become sharper and more intense when the calcination temperature increases from 973 K to 1473 K, implying that the crystallinity of bulk $ZnGa_2O_4$ increases with an increase in the calcination temperature.
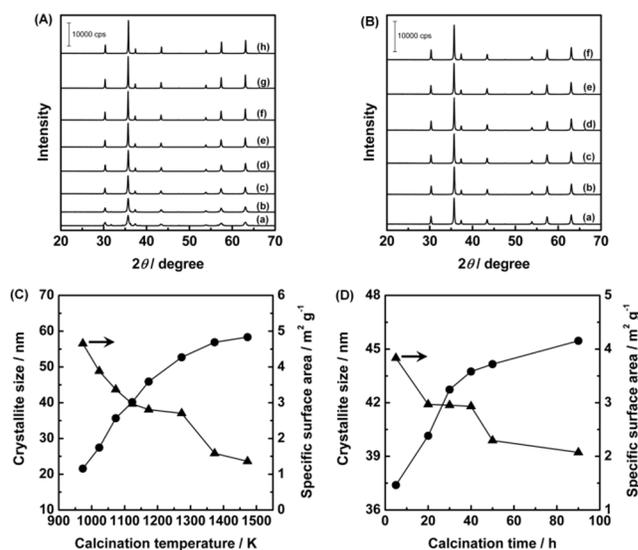

Fig. 1 (A) XRD patterns of $ZnGa_2O_4$ calcined at 973 K (a), 1023 K (b), 1073 K (c), 1123 K (d), 1173 K (e), 1273 K (f), 1373 K (g), and 1473 K (h) for 20 h; (B) XRD patterns of $ZnGa_2O_4$ calcined at 1123 K for 5 h (a), 20 h (b), 30 h (c), 40 h (d), 50 h (e), and 90 h (f); (C) Crystallite size and specific surface area of $ZnGa_2O_4$ calcined at various temperatures for 20 h; (D) Crystallite size and specific surface area of $ZnGa_2O_4$ calcined at 1123 K for different time.

The calcination time also promotes the crystallinity of $ZnGa_2O_4$. As shown in Fig. 1(B), the XRD patterns for $ZnGa_2O_4$ samples that were calcined at 1123 K for 5 h to 90 h show a slight increase in peak intensity. In addition, the increased crystallinity of $ZnGa_2O_4$ is indicated by the larger crystallite size. The crystallite size of $ZnGa_2O_4$ can be measured using Scherrer's equation, $D = K \lambda / (B \cos \theta)$. Here, K is a constant (0.9), λ is the wavelength of Cu Kα

radiation, B is the Full Width of Half Maximum (FWHM) of the diffraction peak centered at 35.7°, and θ is the scattering angle.[20] Fig. 1(C) shows that the crystallite size of $ZnGa_2O_4$ calcined at temperatures ranging from 973 K to 1473 K increased gradually from 21.5 nm to 58.3 nm. Conversely, the specific surface area of $ZnGa_2O_4$ samples, which was measured by the BET method, decreases as the calcination temperature is elevated. Similarly, a small increase in the crystallite size and a small reduction in the BET surface area with longer calcination time are observed in Fig. 1(D). These results show that calcination at various temperatures for different times affects not only the crystallite size, but also their specific surface area.
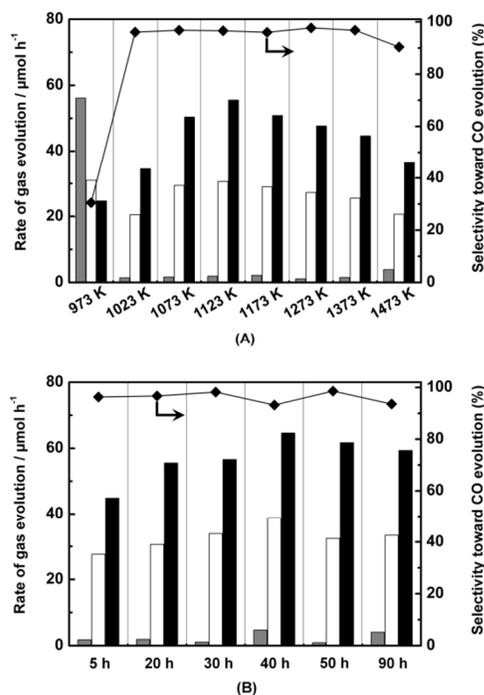

(A)

(B)

Fig. 2 (A) Rates of CO (black), O_2 (white), and H_2 (gray) evolution and selectivity to CO evolution over $ZnGa_2O_4$ calcined at various temperatures for 20 h; (B) Rates of CO (black), O_2 (white), and H_2 (gray) evolution and selectivity to CO evolution over $ZnGa_2O_4$ at 1123 K for different time. Ag cocatalyst was modified by the photodeposition method and the loading amount was 1.0 wt%. Amount of catalyst under photoirradiation using a 400 W high-pressure mercury lamp: 1.0 g, volume of water: 1.0 L, CO_2 flow rate: 30 mL min^{-1}, additve: $NaHCO_3$ (0.1 mol L^{-1}).

It is known that the photocatalytic activity of the catalyst is dependent on its the crystallinity and specific surface area.[12,21] This is because the photocatalytic reaction occurs mainly on the surface of the photocatalyst, and high crystallinity with the decreased density of defects in the photocatalyst provides smooth photo-generated charge separation without recombination.[17,18] However, calcination temperature and time promote the crystallization of the photocatalyst and simultaneously diminish the surface area. The balance between crystallization and specific surface area must be finely tuned to obtain the maximum photocatalytic activity. Thus, the activities for the photocatalytic conversion of CO_2 by H_2O under UV irradiation of $ZnGa_2O_4$ catalysts prepared under different conditions were compared. Fig. 2(A) shows the formation rates of CO, O_2 and H_2, and the selectivity toward CO evolution with $ZnGa_2O_4$ calcined at various temperatures for 20 h. The surfaces of all the samples were modified with Ag by the photodeposition method. All the Ag/$ZnGa_2O_4$ photocatalysts produced CO as a main reduction product and significantly suppressed the production of H_2, except for

the sample sintered at 973 K. According to the XRD patterns, the impurity in this particular $ZnGa_2O_4$ structure may be responsible for the much higher yield of H_2. Thus, the selectivity toward CO evolution over H_2 evolution on $ZnGa_2O_4$ with a pure spinel phase was stable above 90%. The simultaneous stoichiometric evolution of O_2 confirmed that H_2O functions as an electron donor and consumes the photo-holes generated during the photocatalytic conversion of CO_2. The evolution of CO over Ag-modified $ZnGa_2O_4$ was improved with an increase in the calcination temperature from 973 K to 1123 K, which can be attributed to the increased crystallinity of the $ZnGa_2O_4$, despite the decrease in its specific surface area. The highest rate of CO evolution was obtained over $ZnGa_2O_4$ calcined at 1123 K. However, the formation rate of CO declined with an increase in the calcination temperatures beyond 1123 K due to the diminishing surface area of the $ZnGa_2O_4$ catalyst. As with the calcination temperature, the increase of calcination time from 5 h to 90 h also influenced the activity of the $ZnGa_2O_4$ (Fig. 2(B)). The incremental crystallite size of $ZnGa_2O_4$ heated at 1123 K from 5 h to 40 h resulted in the promotion of CO evolution. Further increase in the calcination time led to a slight increase in crystallite size and a slight decrease in surface area, thus the formation rate of CO did not drop significantly. It is noteworthy that $ZnGa_2O_4$ calcined at 1123 K for 40 h had the optimized balance of crystallite size and specific surface area, and exhibited the good activity (64.6 μmol h^{-1} of CO) for the photocatalytic conversion of CO_2 with H_2O.
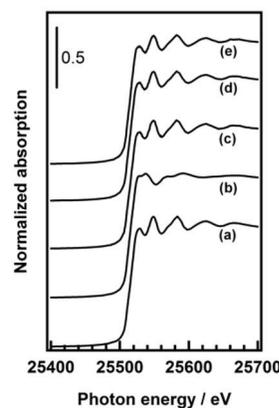

Fig. 3 Ag K-edge XANES spectra of Ag foil (a), Ag_2O (b), and the Ag-modified $ZnGa_2O_4$ prepared by the photodeposition method (c), impregnation method (d), and chemical reduction method (e). $ZnGa_2O_4$ was calcined at 1123 K for 40 h and the loading amount of Ag was 1.0 wt%.
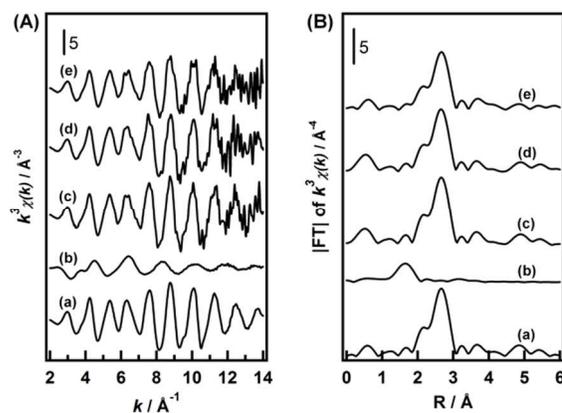

Fig. 4 Ag K-edge EXAFS (A), and Fourier transforms (FT) of EXAFS (B) spectra of Ag foil (a), Ag_2O (b), and the Ag-modified $ZnGa_2O_4$ prepared by the photodeposition method (c), impregnation method (d), and chemical reduction method (e). $ZnGa_2O_4$ was calcined at 1123 K for 40 h and the loading amount of Ag was 1.0 wt%.

Ag metal has been employed as an effective electrode in the electrochemical reduction of CO_2 for CO production.[22] The modification of the surface of $ZnGa_2O_4$ with a Ag cocatalyst also has a significant effect on the photocatalytic conversion of CO_2 with H_2O. Fig. 3 and 4 show the Ag K-edge XANES, EXAFS, and Fourier transforms (FT) of EXAFS spectra of Ag-modified $ZnGa_2O_4$ prepared by photodeposition, impregnation and chemical reduction methods. The XANES spectral shape of the three samples was similar to that of Ag foil (Fig. 3), indicating that all Ag species loaded by the three methods are metallic. Moreover, the same characteristic distance of Ag-Ag shell peaks for the three photocatalysts and Ag foil in the FT of EXAFS spectra (Fig. 4) confirm that Ag metal is present on the $ZnGa_2O_4$. However, the height of the Ag-Ag shell peak of $ZnGa_2O_4$ Ag-modified by the chemical reduction method was lower than those of the samples synthesized by the photodeposition and impregnation methods, indicating that the particle size of the Ag cocatalyst in the chemical reduction sample is the smallest among the three samples.
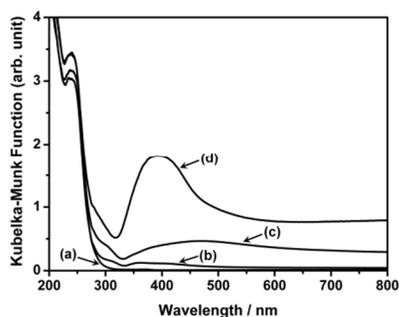

Fig. 5 UV-Vis DRS of bare $ZnGa_2O_4$ (a), and the Ag-modified $ZnGa_2O_4$ prepared by the photodeposition method (b), impregnation method (c), and chemical reduction method (d). $ZnGa_2O_4$ was calcined at 1123 K for 40 h and the loading amount of Ag was 1.0 wt%.
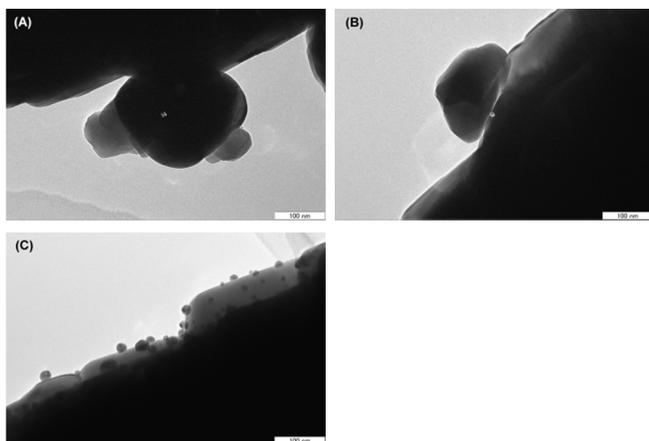

Fig. 6 TEM images of Ag-modified $ZnGa_2O_4$ prepared by photodeposition method (A), impregnation method (B), and chemical reduction method (C). $ZnGa_2O_4$ was calcined at 1123 K for 40 h and the loading amount of Ag was 1.0 wt%.

The UV-Vis DRS of bare $ZnGa_2O_4$ and Ag-modified $ZnGa_2O_4$ loaded by the three methods are shown in Fig. 5. The absorption edge of bare $ZnGa_2O_4$ is located at 270 nm and the band gap energy of $ZnGa_2O_4$ is estimated to be 4.67 eV by Davis–Mott's equation.[23] All the Ag-modified $ZnGa_2O_4$ samples exhibit the same intrinsic absorption as bare $ZnGa_2O_4$. A strong surface plasmon absorption at around 400 nm and a wide absorption in the visible and near-infrared region are observed for the Ag-modified $ZnGa_2O_4$ prepared by the chemical reduction method, indicating that small Ag particles are

densely dispersed on the surface of the $ZnGa_2O_4$.[24] For Ag-modified $ZnGa_2O_4$ fabricated by photodeposition and impregnation methods, weak surface plasmon absorptions can be attributed to the aggregation and poor dispersion of Ag particles. Fig. 6 shows the TEM images of Ag-modified $ZnGa_2O_4$ prepared by the three methods. Clearly, the chemical reduction method affords highly dispersed Ag particles with a narrow particle size distribution in comparison with the photodeposition and wet impregnation methods. This observation is consistent with the results of the XAFS and UV-Vis DRS experiments.
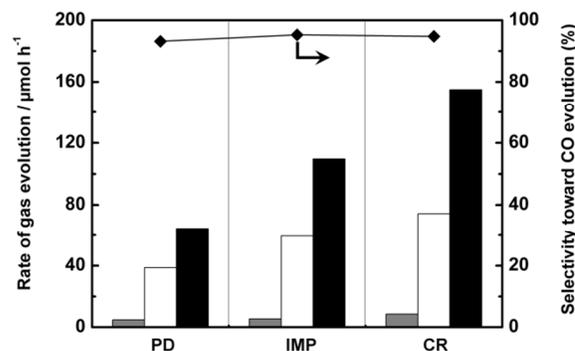

Fig. 7 Rates of CO (black), O_2 (white), and H_2 (gray) evolution and selectivity to CO evolution over Ag-modified $ZnGa_2O_4$ prepared by PD (photodeposition method), IMP (impregnation method), and CR (chemical reduction method). $ZnGa_2O_4$ was calcined at 1123 K for 40 h and the loading amount of Ag was 1.0 wt%. Amount of catalyst under photoirradiation using a 400 W high-pressure mercury lamp: 1.0 g, volume of water: 1.0 L, CO_2 flow rate: 30 mL min^{-1}, additve: $NaHCO_3$ (0.1 mol L^{-1}).
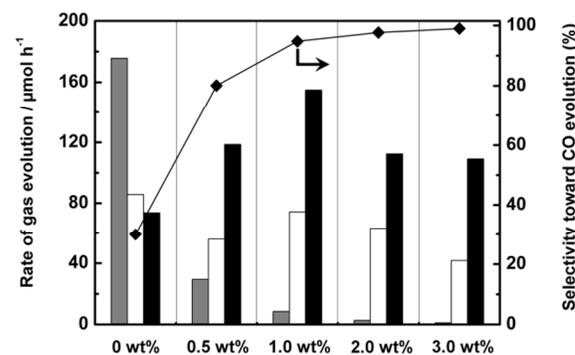

Fig. 8 Rates of CO (black), O_2 (white), and H_2 (gray) evolution and selectivity to CO evolution over Ag-modified $ZnGa_2O_4$ with different Ag contents. $ZnGa_2O_4$ was calcined at 1123 K for 40 h. Ag cocatalyst was modified by chemical reduction method. Amount of catalyst under photoirradiation using a 400 W high-pressure mercury lamp: 1.0 g, volume of water: 1.0 L, CO_2 flow rate: 30 mL min^{-1}, additve: $NaHCO_3$ (0.1 mol L^{-1}).

Fig. 7 shows how the photocatalytic conversion of CO_2 by H_2O is affected by the Ag-modification method employed in the preparation of the catalyst. It can be seen that CO, H_2, and O_2 are evolved in stoichiometric amounts over the $ZnGa_2O_4$ modified by all three methods, and that the selectivity toward CO evolution was similar in each case. Due to the formation of metallic Ag nanoparticles with small size and good dispersion on the $ZnGa_2O_4$, the $ZnGa_2O_4$ modified by the chemical reduction method exhibits significantly enhanced photocatalytic activity for the conversion of CO_2 to CO.

The effect of the amount of Ag cocatalyst loaded onto the catalyst on the evolution of CO is shown in Fig. 8. Conversion of CO_2 to CO can take place on bare $ZnGa_2O_4$, but in that case the formation rate of H_2 (175.7 µmol h^{-1}) is higher than that of CO (73.7

µmol h^{-1}). The total photocatalytic activity of the bare $ZnGa_2O_4$ was high, whereas the selectivity toward CO evolution was quite low. This is because the number of suitable reaction sites for the reduction of CO_2 is insufficient on the surface of the highly crystalline $ZnGa_2O_4$, and the water-splitting reaction competes with the reduction of CO_2 for these reaction sites. The modification of $ZnGa_2O_4$ with a Ag cocatalyst causes a dramatic increase in the photocatalytic activity for the evolution of CO. While the formation rate of CO increases with the addition of larger amounts of Ag from 0 to 1.0 wt%, the rate declines with further loading of Ag. The maximum activity is obtained with $ZnGa_2O_4$ loaded with 1 wt% of the Ag cocatalyst. Conversely, the production of H_2 steadily decreases with an increase in Ag loading, thus the selectivity for CO over H_2 increases and reaches 99.0%. It is clear that the surface modification of the photocatalyst efficiently changes the selectivity toward CO evolution. The introduction of an Ag cocatalyst provides enough catalytic sites for the reduction of CO_2 on the surface of $ZnGa_2O_4$, therefore the conversion of CO_2 to CO takes precedence over the production of H_2 at such sites.
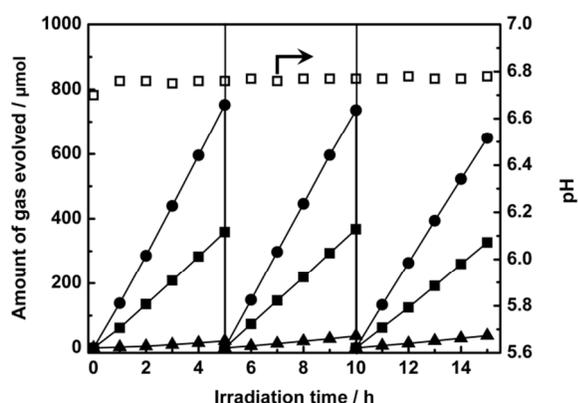

Fig. 9 Time courses of CO (circle), O_2 (square), and H_2 (triangle) evolutions for the photocatalytic conversion of CO_2 by H_2O over Ag-modified $ZnGa_2O_4$. $ZnGa_2O_4$ was calcined at 1123 K for 40 h. Ag cocatalyst was modified by chemical reduction method and the loading amount was 1.0 wt%. Amount of catalyst under photoirradiation using a 400 W high-pressure mercury lamp: 1.0 g, volume of water: 1.0 L, CO_2 flow rate: 30 mL min^{-1}, additve: $NaHCO_3$ (0.1 mol L^{-1}).
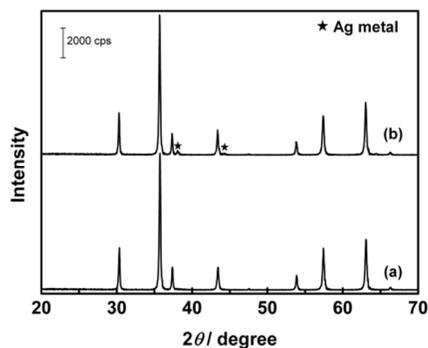

Fig. 10 XRD patterns of Ag-modified $ZnGa_2O_4$ before (a) and after (b) the 15h reaction. $ZnGa_2O_4$ was calcined at 1123 K for 40 h. Ag cocatalyst was modified by chemical reduction method and the loading amount was 1.0 wt%.

The time course of CO, H_2, and O_2 evolution during the photocatalytic conversion of CO_2 by H_2O over Ag-modified $ZnGa_2O_4$ under optimized conditions is shown in Fig. 9. CO is evolved as a main reduction product, and only a very small amount of H_2 is generated. Simultaneously, the evolution of O_2 increases linearly during the reaction. The formation rates of CO, H_2, and O_2

(155, 8.5 and 74.3 µmol h^{-1}, respectively) are in an approximately stoichiometric ratio, indicating that the number of photogenerated electrons used in the reduction of CO_2 and protons is equivalent to that of holes consumed by the oxidation of H_2O. After 5 h of photoirradiation, we obtained 752 µmol of CO, 21.7 µmol of H_2, and 359 µmol of O_2. The reaction was repeated three times, and the evolution of CO slightly decreased on the third run.

The XRD patterns of Ag-modified $ZnGa_2O_4$ before and after the photocatalytic reaction shown in Fig. 10 indicate that the crystalline structure of $ZnGa_2O_4$ is very stable under UV light irradiation and in aqueous medium. A diffraction peak assigned to the metallic Ag appears in the case of Ag-modified $ZnGa_2O_4$ after the reaction, indicating that the Ag particles undergo aggregation under photoirradiation. Moreover, the coalesced Ag particles after the reaction are distinct in the TEM images, as shown in Figure S2. It is believed that the change in the particle size of the Ag cocatalyst, which is caused by the redeposition and aggregation of Ag species on the $ZnGa_2O_4$ during photoirradiation, is responsible for the decrease in evolution of CO in the long-duration reaction. It is important to maintain the small particle size and uniform dispersion of the metallic Ag cocatalyst during the conversion of CO_2 in H_2O, and investigation of this phenomenon is currently underway in our group in order to improve the activity and stability of the Ag-modified photocatalysts.
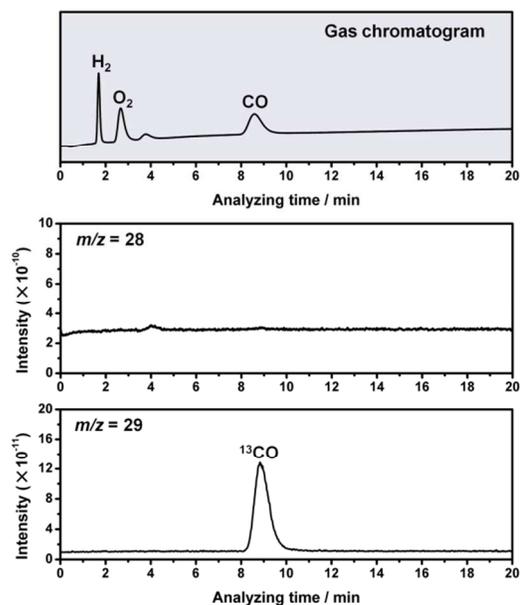

Fig. 11 Gas chromatogram and mass spectra (m/z 28 and 29) in the photocatalytic conversion of $^{13}CO_2$ by H_2O over Ag-modified $ZnGa_2O_4$. $ZnGa_2O_4$ was calcined at 1123 K for 40 h. Ag cocatalyst was modified by chemical reduction method and the loading amount was 1.0 wt%. Amount of catalyst under photoirradiation using a 400 W high-pressure mercury lamp: 1.0 g, volume of water: 1.0 L, CO_2 flow rate: 30 mL min^{-1}, additve: $NaHCO_3$ (0.1 mol L^{-1}).

In the photocatalytic conversion of CO_2, any organic contamination could result in the misestimating of carbon-containing products. Although the residual carbon species on the $ZnGa_2O_4$ surface can be eliminated during the high-temperature fabrication process, it is important to confirm the carbon source of the gas products, which we have done through an isotope-labeling experiment using $^{13}CO_2$. Fig. 11 shows the mass spectra (m/z 28 and 29) during the photocatalytic conversion of $^{13}CO_2$ by H_2O over $ZnGa_2O_4$ modified with Ag by the chemical reduction method. Sampled gases were introduced to the mass spectrometer after separation by gas chromatography. The peak in the spectrum of m/z

= 29, which is attributed to the ^{13}CO gas, appears at the same retention time as that monitored by GC. This result shows that the CO evolved over Ag-modified $ZnGa_2O_4$ originates from the introduced CO_2 gas.

Conclusions

Ag-modified $ZnGa_2O_4$ exhibits high activity and selectivity toward CO evolution in the photocatalytic conversion of CO_2 by H_2O. The stoichiometric evolution of O_2 observed proves that H_2O can function efficiently as an electron donor during the photocatalytic conversion of CO_2. The crystallinity of the $ZnGa_2O_4$ catalyst increases, and the surface area decreases, with increasing calcination temperature and time. The maximum amount of CO is produced over $ZnGa_2O_4$ calcined at 1123 K for 40 h. Modification of the catalyst with an Ag cocatalyst by the chemical reduction method also improves the photocatalytic activity of $ZnGa_2O_4$. Thus, 155.0 μmol h^{-1} of CO, 8.5 μmol h^{-1} of H_2, and 74.3 μmol h^{-1} of O_2 were obtained using Ag-modified $ZnGa_2O_4$ under optimized conditions. An isotope-labeling reaction using $^{13}CO_2$ provided evidence that the carbon source of evolved CO is not residual carbon species on the photocatalyst surface, but is the CO_2 introduced in the gas phase.

Acknowledgement

References

1　J. Hansen, L. Nazarenko, R. Ruedy, M. Sato, J. Willis, A. D. Genio, D. Koch, A. Lacis, K. Lo, S. Menon, T. Novakov, J. Perlwitz, G. Russell, G. A. Schmidt and N. Tausnev, *Science*, 2005, **308**, 1431.

2　M. Mikkelsen, M. Jorgensen and F. C. Krebs, *Energy Environ. Sci.*, 2010, **3**, 43.

3　E. V. Kondratenko, G. Mul, J. Baltrusaitis, G. O. Larrazábal and J. Pérez-Ramírez, *Energy Environ. Sci.*, 2013, **6**, 3112.

4　G. Centi, E. A. Quadrelli and S. Perathoner, *Energy Environ. Sci.*, 2013, **6**, 1711.

5　A. Kubacka, M. Fernández-García and G. Colón, *Chem. Rev.*, 2012, **112**, 1555.

6　F. Fresno, R. Portela, S. Suárezc and J. M. Coronado, *J. Mater. Chem. A*, 2014, **2**, 2863.

7　J. Mao, K. Li and T. Y. Peng, *Catal. Sci. Technol.*, 2013, **3**, 2481.

8　W. Q. Fan, Q. H. Zhang and Y. Wang, *Phys. Chem. Chem. Phys.*, 2013, **15**, 2632.

9　K. Li, A. D. Handoko, M. Khraisheh and J. W. Tang, *Nanoscale*, 2014, **6**, 9767.

10　K. Teramura, Z. Wang, S. Hosokawa, Y. Sakata and T. Tanaka, *Chem. −Eur. J.*, 2014, **20**, 9906.

11　K. Iizuka, T. Wato, Y. Miseki, K. Saito and A. Kudo, *J. Am. Chem. Soc.*, 2011, **133**, 20863.

12　Z. Wang, K. Teramura, S. Hosokawa and T. Tanaka, *Appl. Catal. B*, 2015, **163**, 241.

13　K. Ikarashi, J. Sato, H. Kobayashi, N. Saito, H. Nishiyama and Y. Inoue, *J. Phys. Chem. B*, 2002, **106**, 9048.

14　S. C.Yan, S. X. Ouyang, J. Gao, M. Yang, J. Y. Feng, X. X. Fan, L. J. Wan, Z. S. Li, J. H. Ye, Y. Zhou and Z. G. Zou, *Angew. Chem., Int. Ed.*, 2010, **49**, 6400.

15　S. C. Yan, J. J. Wang, H. L. Gao, N. Y. Wang, H. Yu, Z. S. Li, Y. Zhou and Z. G. Zou, *Adv. Funct. Mater.*, 2013, **23**, 758.

16　Q. Liu, D. Wu, Y. Zhou, H. B. Su, R. Wang, C. F. Zhang, S. C. Yan, M. Xiao and Z. G. Zou, *ACS Appl. Mater. Interfaces*, 2014, **6**, 2356.

17　K. Maeda and K. Domen, *J. Phys. Chem. C*, 2007, **111**, 7851.

18　M. Kitano and M. Hara, *J. Mater. Chem.*, 2010, **20**, 627.

19　K. Shimura and H. Yoshida, *Phys. Chem. Chem. Phys.*, 2012, **14**, 2678.

20　I. Papadas, J. A. Christodoulides, G. Kioseoglou and G. S. Armatas, *J. Mater. Chem. A*, 2015, **3**, 1587.

21　A. Kudo and Y. Miseki, *Chem. Soc. Rev.*, 2009, **38**, 253.

22　Y. Hori, K. Kikuchi and S. Suzuki, *Chem. Lett.*, 1985, **14**, 1695.

23　V. B. R. Boppana, D. J. Doren and R. F. Lobo, *J. Mater. Chem.*, 2010, **20**, 9787.

24　K. H. Chen, Y. C. Pu, K. D. Chang, Y. F. Liang, C. M. Liu, J. W. Yeh, H. C. Shih and Y. J. Hsu, *J. Phys. Chem. C*, 2012, **116**, 19039.

^{a}*Department of Molecular Engineering, Graduate School of Engineering, Kyoto University, Kyoto 615-8510, Japan.*
^{b}*Elements Strategy Initiative for Catalysts & Batteries (ESICB), Kyoto University, Kyotodaigaku Katsura, Nishikyo-ku, Kyoto 615–8520, Japan.*
^{c}*Precursory Research for Embryonic Science and Technology (PRESTO), Japan Science and Technology Agency (JST), 4-1-8 Honcho, Kawaguchi, Saitama 332-0012, Japan.*